EUROPEAN ORGANIZATION FOR NUCLEAR RESEARCH

CERN/MPS/LIN 72-1
8 March 1972

A CRITICAL STUDY OF EMITTANCE MEASUREMENTS OF INTENSE LOW-ENERGY PROTON BEAMS

L.R. Evans and D.J. Warner
CERN, Geneva, Switzerland

1. INTRODUCTION

In proton linacs considerable improvement has been made in recent years in beam diagnostics and measurements. In particular, it is now possible in many laboratories to do automatic measurements of the beam transverse phase-space density distribution[1]. This has made possible more detailed comparisons of the measured dynamics with theory and computations than previously[2].

Most of the methods used to measure emittance and current density in the range 500 keV to 50 MeV are essentially variants of the same basic technique, i.e. a metallic plate containing small slits or holes defines positions in the beam real space, followed by an analysing and detection system relying on a drift to produce spatial variations corresponding to the angular divergences in the beam. More sophisticated applications of this method include focusing between defining plate and analyser, multiple collecting electrodes at the analyser, single pulse measurements, and computer control and automatic data collection. All of the methods reported are subject to two effects which, depending on current density, emittance, and beam energy may produce significant perturbation of the beam during the measurement.

i) Space-charge effects between defining and analysing apparatus perturb the simple linear drift matrix usually assumed, and may result in a beam size at the analyser considerably larger than that due to emittance alone. This sets an upper limit to the size of defining slit and drift distance which may be used, and is discussed in more detail below.

ii) It has recently been pointed out[3,4] that for low-energy proton beams (< 1 MeV) the large fraction of the beam stopped at the first defining plate may liberate secondary electrons which can stream back along the beam thus perturbing the dynamics during the measurement. In effect the beam may become almost completely neutralized (locally) during the measurement, and may therefore record completely different density and emittance characteristics to those of the beam which is transported through the system. A large part of this paper is devoted to an experimental study of the magnitude of this effect

in a 500 keV proton beam at the CERN 3 MeV experimental linac, and a comparison of the results with dynamics computations. During this work it was found that the percentage noise level on samples of the beam when using slits or apertures was always considerably higher than on the total beam pulse. This effectively limited the resolution of the measurements and therefore merits further discussion below.

2. SPACE CHARGE BLOW-UP IN STRIP BEAMS

In the emittance measurements described later, a simple two-slit method is used. To estimate the effect of space charge on the blow-up of the ribbon of beam passing between defining and analysing slits, we treat the limiting case of an infinite strip of constant current density J_0 and initial width $2y_0$ at S = 0

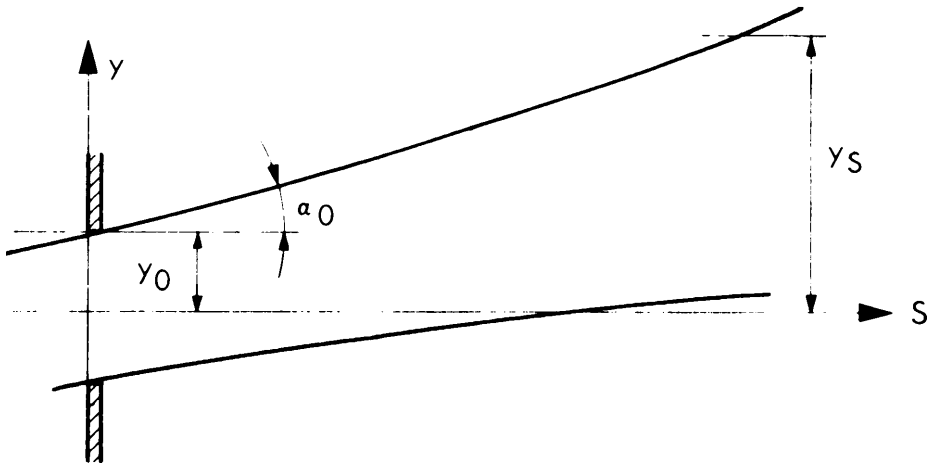

At the beam edge the y-component of the electric field is given by Gauss' theorem:

$$E_y = \frac{\rho(y)\, y}{\varepsilon_0} = \frac{J_0\, y_0}{\varepsilon_0\, v_S} \,. \qquad (1)$$

The transverse force is thus

$$\frac{d^2y}{dt^2} = \frac{eE_y}{m} \qquad (2)$$

which transforms to the envelope equation (for laminar flow, i.e. no emittance):

$$\frac{d^2y}{dS^2} = k\, J_0\, y_0 \ , \tag{3}$$

with $k = e/(M\, \varepsilon_0\, v_S^3) = 1.122 \times 10^{-2}$ MKS units at 500 keV.

Integrating Eq. (3) twice, we obtain

$$y(S) = \frac{k}{2} J_0\, y_0\, S^2 + \alpha_0 S + y_0 \ , \tag{4}$$

with α_0 the angle made by the beam edge with the axis at S = 0. The term on the r.h.s. of Eq. (4) may be used to quantify our discussion. If $J_0 = 0$ and we now allow a spread of initial angles $\alpha_0 \pm \Delta\alpha/2$ over the slit width (finite emittance), then the angular resolution can be given as

$$\Delta_r\alpha = 2y_0/S \ , \tag{5}$$

and usually one has $\Delta\alpha >> \Delta_r\alpha$ for precise emittance measurements.

Suppose one requires that the emittance term be greater than the space-charge term:

$$\frac{\Delta\alpha}{2} S > \frac{k\, J_0}{2} y_0\, S^2 \ . \tag{6}$$

With typical values of emittance = 100 π mm•mrad, beam radius = 10 mm, angular divergence $\Delta\alpha/2$ = 10 mrad, current = 300 mA, Eq. (6) can be written

$$y_0\, S < 2 \times 10^{-3}\ m^2 \tag{7}$$

which is not a very tight limitation.

Another tighter condition that one can apply is that the angular blow-up due to space-charge be too small to be resolved, i.e.

$$\frac{k\, J_0}{2} y_0\, S^2 \leq \Delta\alpha_r\, S \ . \tag{8}$$

With the same values as above, the inequality (8) becomes

$$S \leq 0.63 \text{ m} . \tag{9}$$

Thus to retain a good angular resolution and yet reduce the space-charge effect, one should reduce both y_0 and S to satisfy both of the above inequalities. One may then be limited by current detector sensitivity and noise on the beam pulse, so a compromise is required. In our experiments we have used $y_0 \leq 0.2$ mm, S = 0.526 m, which according to the inequality (8) should give precise results for $J_0 \leq 0.65$ mA/mm^2.

3. RELATIVE IMPORTANCE OF SPACE-CHARGE AND EMITTANCE IN GOVERNING BEAM DYNAMICS

In this and previous papers we have several times made allusion to 'beams in which space-charge is important'. For the present measurements it is useful to define precisely a space-charge parameter which ideally is dimensionless and has value unity when space-charge and emittance effects are equal. Historically the often-quoted reference[5] to Kapchinskij and Vladimirskij (1959) provides the basis for our parameter. We write the K-V envelope equations in the form used by Lapostolle[6]:

$$\begin{aligned} a'' + W_y^2 \, a - \frac{E_y^2}{a^3} - \frac{2A}{a+b} &= 0 \\ b'' + W_z^2 \, b - \frac{E_z^2}{b^3} - \frac{2A}{a+b} &= 0 . \end{aligned} \tag{10}$$

a, b are envelope sizes in y, z directions, with the differential made with respect to axial direction S; W_y^2, W_z^2 are the external focusing parameters; E_z, E_y are the phase areas divided by π of the beam in y,y′ and z,z′ phase-space, respectively, and

$$A = \frac{eI}{2\pi \, \varepsilon_0 M_0 c^3 \beta^3 \gamma^3} , \tag{11}$$

with I the beam current and the other parameters having their usual meaning. Thus we can define space-charge parameters for each phase plane:

$$\delta_y = \frac{2A}{E_y^2} \frac{a^3}{(a + b)}$$

$$\delta_z = \frac{2A}{E_z^2} \frac{b^3}{(a + b)} \quad . \tag{12}$$

δ_y, δ_z are equivalent to the space-charge parameters or conditions developed for circular section beams by Lapostolle[6], Garren[7] and Warner[8]. One generalization which we have to make is to equate a, b with $2(\overline{y^2})^{\frac{1}{2}}$, $2(\overline{z^2})^{\frac{1}{2}}$ and set

$$E_y = 4\left[\overline{y^2}\ \overline{y'^2} - (\overline{yy'})^2\right]^{\frac{1}{2}} = 4(\overline{y^2}\ \overline{y'^2})^{\frac{1}{2}}(1 - \rho_{yy'}^2)^{\frac{1}{2}} \quad . \tag{13}$$

At 500 keV,

$$A = 1.833 \times 10^{-3} \text{ I MKS units.}$$

For a 'typical' beam a = b = 10 mm, I = 0.3 A, E = 100 π mm•mrad:

$$\delta = 4.9 \quad .$$

4. SECONDARY ELECTRON EMISSION FROM THE DEFINING APERTURES

Secondary electrons liberated from the defining apertures during the measurements may considerably perturb the proton dynamics, particularly when the secondary emission coefficient is of order unity. For low-energy proton beams a great deal of experimental data and theoretical results are available[9]. In the energy range of interest to us, the secondary electron emission coefficient for proton impact at normal incidence is almost independent of the metal and varies from $\sim$ 4 at 100 keV to $\sim$ 2 at 500 keV and 0.5 at 3 MeV.

Electrons which are stopped by the first defining plate may be accelerated back into the beam and channelled along it by the proton beam space-charge field. One would expect a perturbation of the beam by these electrons when measuring either real space density or emittance when space-charge is important in the dynamics. The secondary electrons can be

suppressed by positively biasing the defining plate. Numerical integration[4] of the Poisson equation shows that this bias must be about three to four times the centre-to-edge beam space-charge potential, e.g. $\sim$ 1500 V to 2000 V for a 500 mA beam at 500 keV. Experiments have been performed to compare emittance and real space density measurements with and without electron suppression, and the results are discussed in the following sections.

5. EXPERIMENTAL DETAILS

Several difficulties were experienced initially when testing the hypothesis that back-streaming electrons perturb emittance measurements. In the drift space between the pre-injector and RF accelerating structure, the gas pressure (mainly hydrogen) is $\sim 2 \times 10^{-4}$ Torr; thus gas neutralization is possible[4]. Also, the hydrogen molecular ion content (H_2^+) of the beam (although probably < 20%) has sensibly different space-charge dynamics and secondary emission characteristics to those of protons. The geometry of the low-energy drift space with a 16 mm aperture beam transformer at the analysing position makes it necessary to use a triplet lens between defining and analysing positions to limit the beam diameter. This could introduce serious aberrations and make interpretation of results less certain.

For the work reported here we have therefore used the 3 MeV experimental area (Fig. 1) where the beam had been analysed, the pressure was low ($\leq 2 \times 10^{-6}$ Torr), and the geometry was both more convenient and controllable and enabled us to eliminate the lens between the apertures and its accompanying aberrations. The principal disadvantage in working in this area was the difficulty in adjusting the transport for the 500 keV beam, since the optics had been designed for 3 MeV. A schematic diagram of the 3 MeV experimental area is shown in Fig. 2 with only components and dimensions relevant to the experimental work included.

5.1 The adjustable apertures

Each set of adjustable apertures (Fig. 3) consists of four tantalum plates 1 mm thick forming, in pairs, slits which move in the vertical (z) or horizontal (y) directions enabling analysis of the beam over a 50 mm square aperture. The plates are supported by invar bars and the mechanical movement is transmitted through vacuum via stainless-steel washer-type bellows.

Stepping motors are used to drive precision threaded rods and hence, via the invar supports, the tantalum plates. Two motors are arranged so that the two plates move together as a fixed-width slit, or so that one plate moves relative to the other to vary the slit width. The slit widths and positions are recorded on a Nixie display via a digital encoder system.

The actual moving parts occupy only 40 mm axial space, although with adapting flanges this length is roughly doubled.

With full beam current, 200 mA for 30 μsec, 1 pps at 3 MeV, there is a dissipation of 20 W to be taken in the worst case on one tantalum plate. In the original design the heat could easily pass by conduction to the support rods. However, when the system was modified to insulate the plates, heat dissipation became a major problem and several insulators were tried with only moderate success before a final design using alumina support blocks was developed.

To avoid errors due to space-charge blow-up of the strip beam, slit widths down to 0.3 mm were necessary. This obviously placed a severe test on the mechanical stability of the system. For each set of measurements the slit width was calibrated by measuring the change in transmitted beam current with observed slit width at the beam centre (where the density was most uniform). This type of measurement gave results for the slit width reproducible to within ±0.1 mm, which anyway was the least significant digit on the Nixie display.

Each plate could be biased separately, and by the same electrical connection the beam current pulse striking the plate could be observed. This facility proved extremely useful for investigating the coherent beam oscillations described below.

6. EXPERIMENTAL RESULTS

6.1 Amplitude oscillations of the sampled beam

A source of continual difficulty which has been encountered in this work is the appearance of a high noise level on the beam pulse when the beam is sampled by slits or small apertures, even though the whole beam pulse measured on a transformer shows little or no oscillation. The degree

of modulation is a function of position across the beam, becoming less at the beam centre and reaching as much as ∿ 50% modulation near the edge. A possible explanation of this effect is that the whole beam is oscillating transversely in a highly coherent way. This was shown to be true by using a pair of the insulated plates as detectors so that each plate intercepted approximately half of the beam. Figure 4a shows two such signals obtained in this way. The oscillations are highly coherent at approximately 770 kHz. Moreover, the two signals are almost exactly 180° out of phase. Figure 4b shows the same signal where the bottom trace is the signal from one single plate whereas the top trace is the sum of the two signals (as would be seen by a beam transformer). The "centre of gravity" of the beam is therefore oscillating transversely, so that when passing through a wide-aperture transformer before a restriction the beam shows little or no noise, whereas after a restriction (such as the buncher aperture or defining slits) the radial oscillation is transformed into a longitudinal density modulation. This type of phenomenon has since been observed at a slightly different frequency (∿ 1 MHz) in the pre-injector region of the 50 MeV injector, and (not surprisingly) a small degree of modulation still remains after acceleration to 50 MeV.

Although the reason for this effect is not completely understood at present, we have found that it can be minimized by adjusting ion source parameters, particularly gas pressure and magnetic field. For the purpose of the emittance measurements, the source was deliberately adjusted in this way to minimize the noise, even though it resulted in a somewhat reduced output current.

6.2 Emittance and real space density measurements

The setting up of the beam transport to the experimental region was rather critical, as the lengths, spacings, and apertures of the magnets at the high-energy end were designed for 3 MeV rather than for 500 keV. The 18 quadrupoles of the Alvarez tank were run in FDFD with the last two adjusted for matching through the bending magnet to the triplet T3. The variable apertures BA4 and BA5 were set to 20 mm × 20 mm squares, and bias (+800 V) was applied to eliminate electrons from the beam whilst it was maximized empirically beyond the second apertures. The duoplasmatron source was adjusted to give a low beam noise at the experiment and this

seemed to lead to a poor percentage transmission ($\sim$ 60%) between tank input and experiment. This could be due to a high H_2^+ content in the beam at this source setting. Without the stability condition, 80% transmission was not uncommon.

Currents were measured 10 μsec from the end of a 35 μsec beam pulse on transformers with a sensitivity of 1.82 mV/mA and a minimum possible resolution of $\sim$ 0.1 mV. This resolution was mainly limited by noise and oscillation on the beam pulse rather than by the gain of the system.

Measurements with and without bias were interleaved throughout; for example, in a real space measurement the calibrated 2.0 mm slit would be set to the initial Y position and the ΔZ = 2.0 mm slit would be scanned in the z-direction in 2 mm steps with bias, then in the reverse direction without bias. Furthermore, after each complete plane had been scanned the checks on summed currents through the slits were made, and measurements were repeated if they did not agree sufficiently well with the total measured current. As far as possible the transformer furthest downstream (BM7) was used for all current measurements as this was much less prone to errors due to back streaming electrons because of the large diameter pipe following and clearing magnet.

For the emittance measurements, defining slits ΔY_1, ΔZ_1 of 0.3 mm were used. The analysing slits ΔY_2, ΔZ_2 were of 2 mm and were moved in 2 mm steps.

The aim of the experiment was to measure the emittances in the Y and Z planes at the front apertures both for biased and earthed defining plates and the real space density at the second set of plates. The measured emittances could then be transferred, using the TRANSPORT program with space-charge [10], to the second position and compared with the measured beam size at this location.

7. RESULTS AND DYNAMICS COMPARISONS

The results of both emittance and real space density measurements were analysed with the emittance analysis program EMITNC [11]. This program fits an analytical function to the data (which can be considered as a two-dimensional histogram). The output consists of equidensity plots

and currents within given emittance areas. In addition, the program computes the r.m.s. parameters of the beam, e.g. $\tilde{y},\tilde{y}'$, and the correlation $\rho_{yy'}$ for the y,y′ plane, both from the raw data and from the fitted function. Some typical equidensity plots are given in Fig. 5, which show the results of real space density measurements with and without bias at the front slit position. Although these results are not used for dynamics comparisons, they show clearly the effect of the secondary electrons leaving the defining plate. Without bias the beam has smaller transverse dimensions and a very peaked current distribution, whereas with bias it is considerably larger and more uniform. A simple picture of electrons entering and neutralizing the beam during the measurement and thereby allowing it to neck down to a smaller diameter seems to apply.

When one compares emittances measured with and without bias (Fig. 6) one notes immediately that the main effect is rotation in phase-space rather like a linear lens plus drift. The current/emittance plots (Figs. 7a and 7b) for these results show that (especially for the y,y′ plane) the total current within a given emittance is not changed to any large extent by this process, as would be expected from a linear system. The continuous curves correspond to two commonly used phase-space distributions, namely constant density (a) and Gaussian (b) in four-dimensional phase space.

In order to decide which was the true beam emittance, the space-charge version of the TRANSPORT program was used to transfer the measured emittances between the two sets of apertures and to compare the effective dimensions $2\tilde{y}$, $2\tilde{z}$ for measured and computed beams at the second location for various assumed beam currents. The results given in Table 1 demonstrate that when biased apertures are used in both positions, the computed and measured results agree well for an effective current of 160 mA. Note that the results of measurements made in the normal manner are in best agreement with the computations if one assumes zero current.

The values of the space-charge parameter shown in the table indicate that for all currents and dimensions of interest in these experiments, space-charge should play the dominant role in the dynamics. Therefore in the unbiased case the beam is neutralized from the front plates during emittance measurements and from the back plates during real space density measurements. It is not surprising that the agreement between computed

and measured values in the unbiased case is not as good as for the biased case, since it is unlikely that the beam is neutralized over the same axial extent from the back plate (BA5) as from the front plate (BA4). Some indication of the axial distance over which neutralization occurs can be obtained by running the dynamics calculation in the reverse direction for the two cases (160 mA and zero current) until the r.m.s. parameters of both beams agree most closely. This distance is about 50 cm, which is approximately the distance between BA4 and the end of the triplet lens.

8. CONCLUSIONS

It has been demonstrated that the normal techniques (i.e. earthed defining apertures) used for these measurements with low-energy beams in which the space-charge parameter is important, severely perturb the beam under observation during the measurement. This makes it impossible to get satisfactory agreement between measured values and computed dynamics unless care is taken to remove the secondary electrons from the beam by the use of biased apertures.

With regard to the experimental difficulties, care should be taken to adjust the defining slit and the drift distance to the analysing slit so that the emittance effect is predominant between the apertures. The beam oscillations which we have observed may be peculiar to our machines, but nevertheless cause serious problems during our measurements and could possibly remain undetected by automatic sampling and measuring systems. Separately insulated aperture plates are obviously essential for detailed emittance and other beam diagnostic studies.

Acknowledgements

Our special thanks are due to A. Bellanger and F. Malthouse for running and maintaining the accelerator, and for assisting with many of the measurements, and to M. Weiss for his constructive criticism of the manuscript. In addition, the authors wish to acknowledge the efforts of many other people who contributed to this work, in particular those concerned with the operation of the ion source and pre-injector and those in the MPS design office and workshops who designed, built, and subsequently modified the variable apertures.

Table 1(a)

Measured beam parameters (Input Data for TRANSPORT)

Input set No.	Aperture bias (V)	$2\tilde{y}$ (mm)	$2\tilde{y}'$ (mrad)	Ey (mm•mrad)	$2\tilde{z}$ (mm)	$2\tilde{z}'$ (mrad)	Ez (mm•mrad)
1	0	6.2	26.0	55	8.3	24.9	74
2	+800	8.3	17.9	54	10.9	15.0	65

Table 1(b)

Comparison of TRANSPORT results and real space measurements

Input set No. [as defined in Table 1(a)]	Input data			Real space measurements		Output results			
	Current (mA)	Space-charge δ_y	Space-charge δ_z	$2\tilde{y}$ (mm)	$2\tilde{z}$ (mm)	$2\tilde{y}$ (mm)	$2\tilde{z}$ (mm)	Space-charge δ_y	Space-charge δ_z
1	0	0	0	8.8	6.1	8.1	6.1	0	0
1	160	3.2	4.2	8.8	6.1	9.0	8.1	8.3	3.3
1	250	5.0	6.6	8.8	6.1	10.2	10.4	15.6	9.1
2	0	0	0	6.3	9.3	3.5	4.8	0	0
2	160	6.0	9.4	6.3	9.3	6.3	9.4	3.2	7.3
2	250	9.4	14.6	6.3	9.3	8.3	11.7	9.0	17.4

REFERENCES

1) Several papers in Session B, Beam diagnostic measurements, Proc. Proton Linear Accelerator Conf., Batavia, 1970 (NAL, Batavia, 1971), vol. 1, p. 107-173.

2) G.W. Wheeler, K. Batchelor, R.L. Gluckstern, J.M. Lefebvre, P.V. Livdahl, D.A. Swenson and C.S. Taylor, Roundtable on performance of new linacs, Proc. Proton Linear Accelerator Conf., Batavia, 1970 (NAL, Batavia, 1971), Vol. 1, p. 99.

3) L.R. Evans and D.J. Warner, Studies of space charge neutralization in intense 500 keV proton beams, IEEE Trans. Nuclear Sci. NS-18, No. 3, 1068 (1971).

4) L.R. Evans and D.J. Warner, Space charge neutralization of intense charged particle beams; some theoretical considerations, CERN/MPS/LIN 71-2 (1971).

5) I.M. Kapchinskij and V.V. Vladimirskij, Limitations of proton beam current in a strong focusing linear accelerator associated with the beam space charge, Proc. Int. Conf. on High-Energy Accelerators and Instrumentation, Geneva, 1959 (CERN, Geneva, 1959), p. 274.

6) P.M. Lapostolle, Quelques propriétés essentielles des effets de la charge d'espace dans des faisceaux continus, CERN/ISR/DI 70-36 (1970).

7) A.A. Garren, Thin lens optics with space charge, Proc. Int. Conf. on High-Energy Accelerators, Yerevan, 1969 (Yerevan Physics Inst., Yerevan, 1970), Vol. 2, p. 415.

8) D.J. Warner, Thesis (unpublished), Univ. of London (1965), p. 25.

9) M. Kaminsky, Atomic and ionic impact phenomenon (Springer-Verlag, Berlin, 1965).

10) F.J. Sacherer and T.R. Sherwood, The effect of space charge in beam transport lines, IEEE Trans. Nuclear Sci., NS-18, No. 3, 1066 (1971).

11) C.S. Taylor, D.J. Warner, F. Block and P. Têtu, Progress Report on the CERN-PS Linac, Proc. Linear Accelerator Conf., Los Alamos, 1966 (Atomic Energy Commission, Washington, 1966), p. 48.

Distribution (open)

ISR, MPS, and SI Scientific Staff

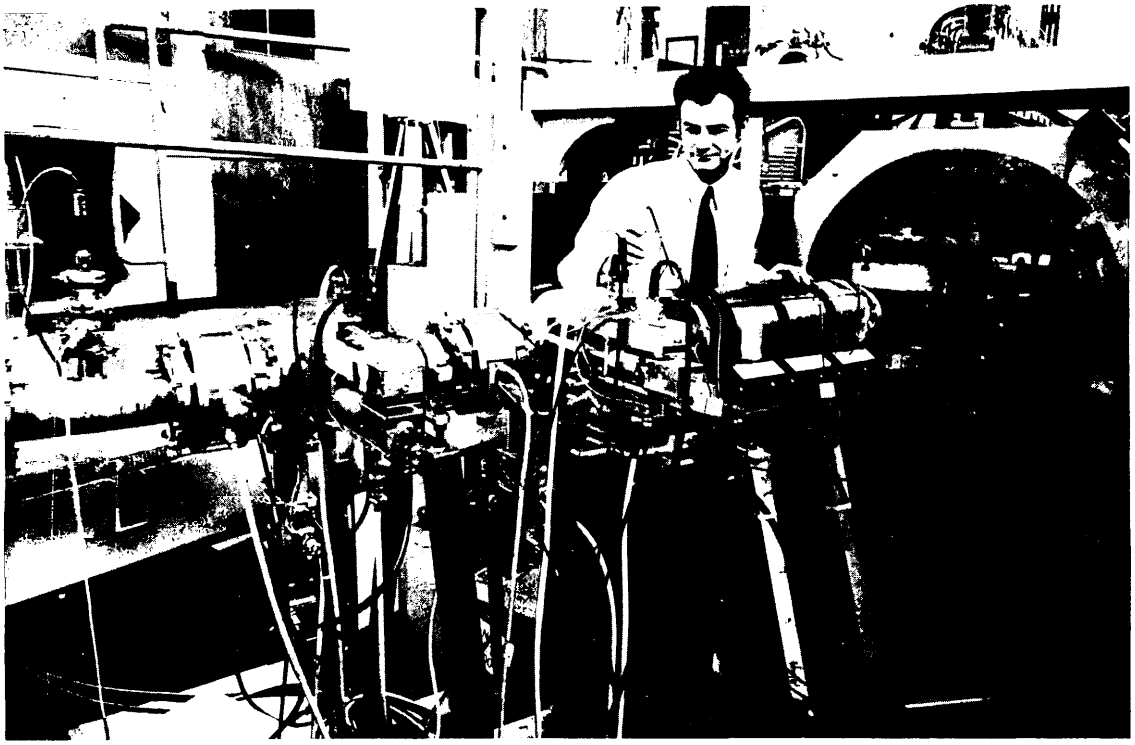

Fig. 1 View of 3 MeV experimental area showing region between accelerating tank and BM7

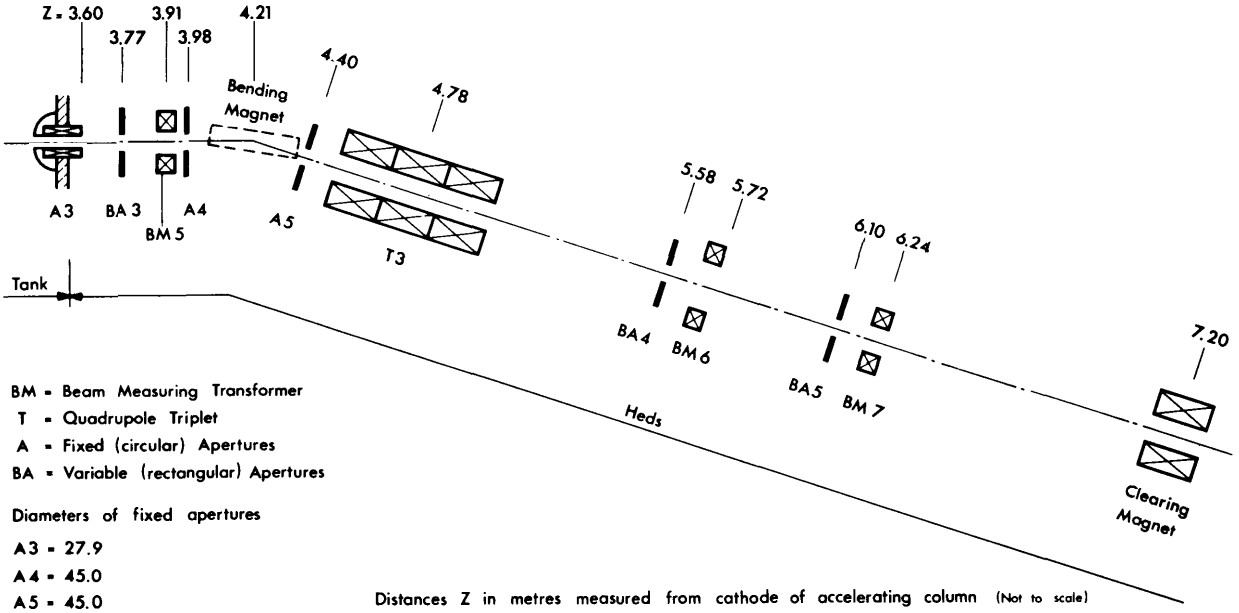

Fig. 2 Schematic diagram of 3 MeV experimental area

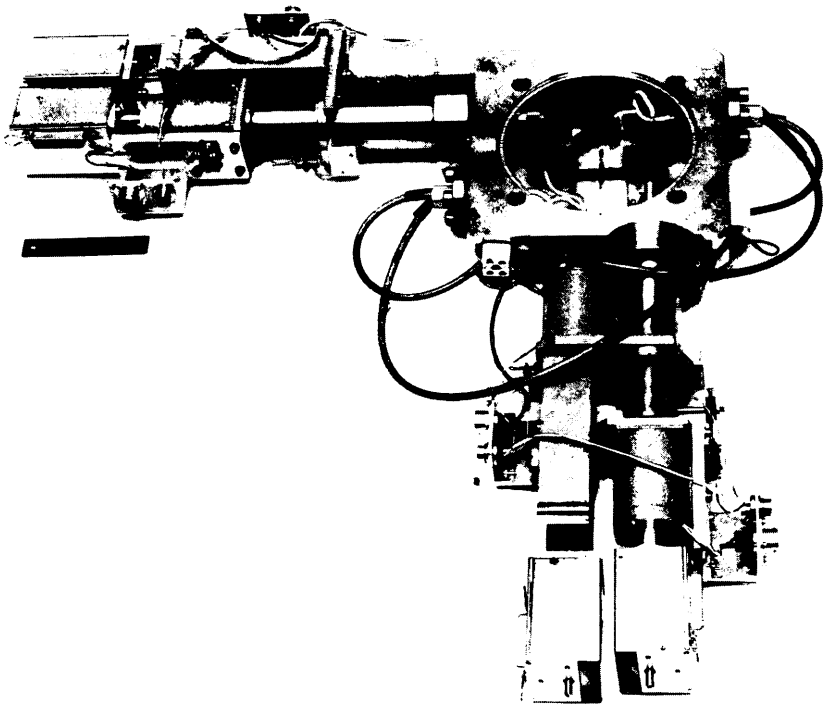

Fig. 3a General view of adjustable aperture assembly

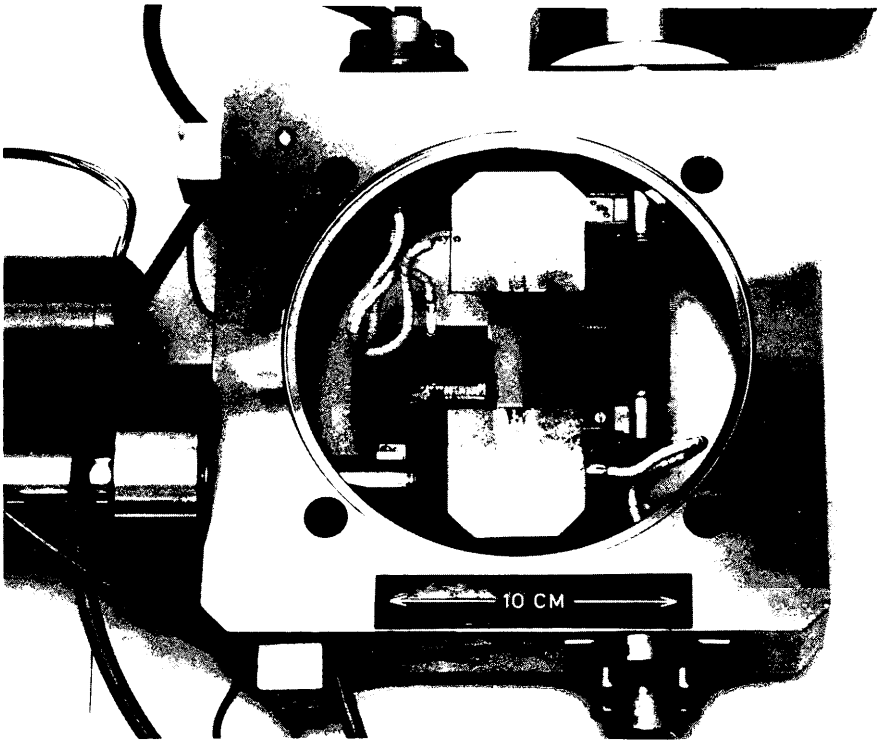

Fig. 3b Details of aperture

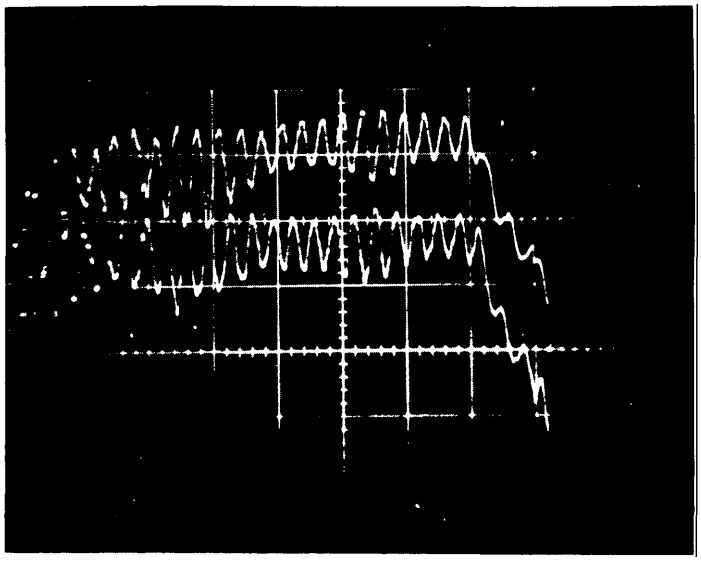

Fig. 4a Beam current signals collected on insulated plates (4 μsec/div, 2 V/div)

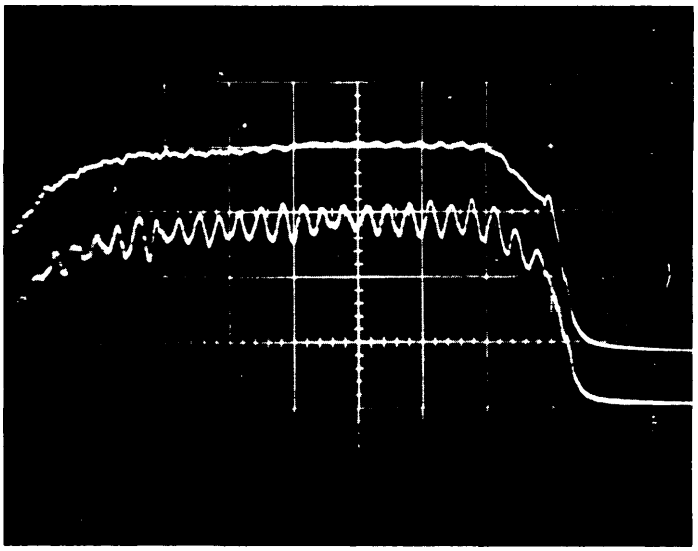

Fig. 4b Sum signal (top, 10 V/div) compared to signal from one plate (bottom, 5 V/div)

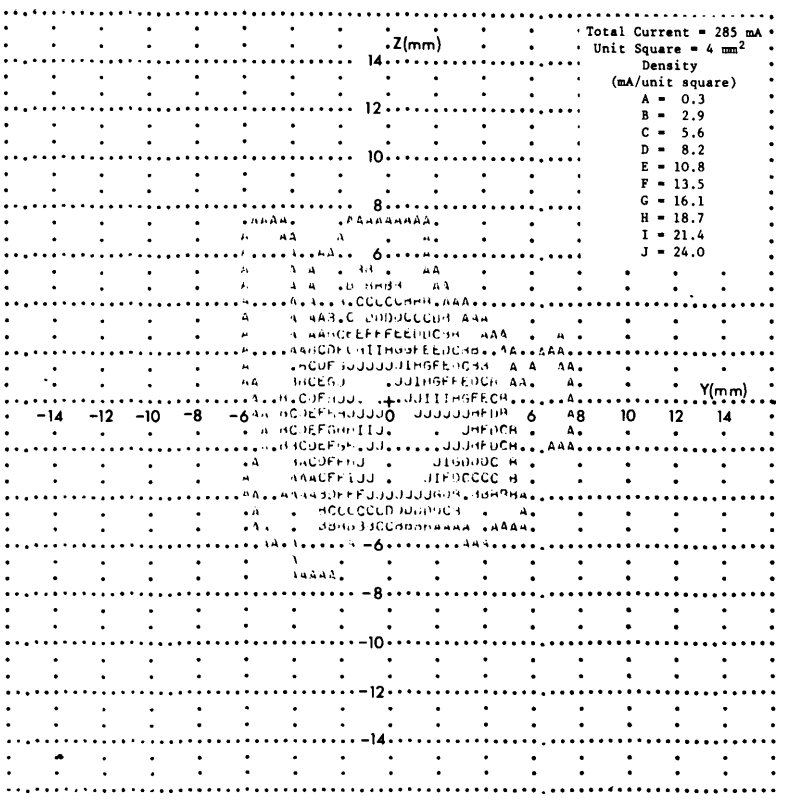

Fig. 5 Equidensity plot for real plane (Y-Z)
a) Bias = 0 V; b) Bias = +800 V

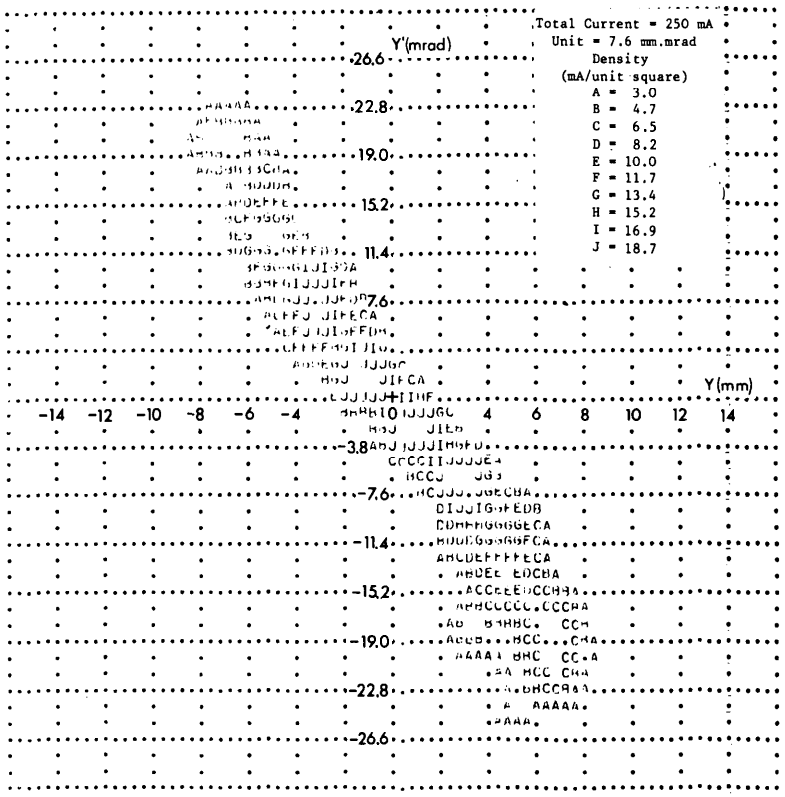

a)

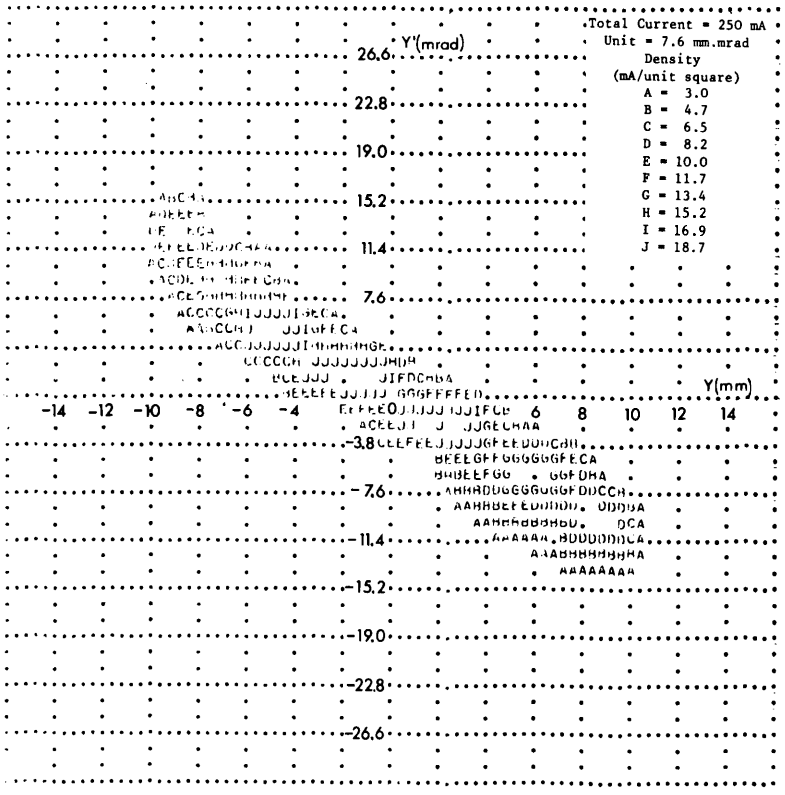

b)

Fig. 6 Equidensity plot for Y-Y′ plane
a) Bias = 0 V; b) Bias = +800 V

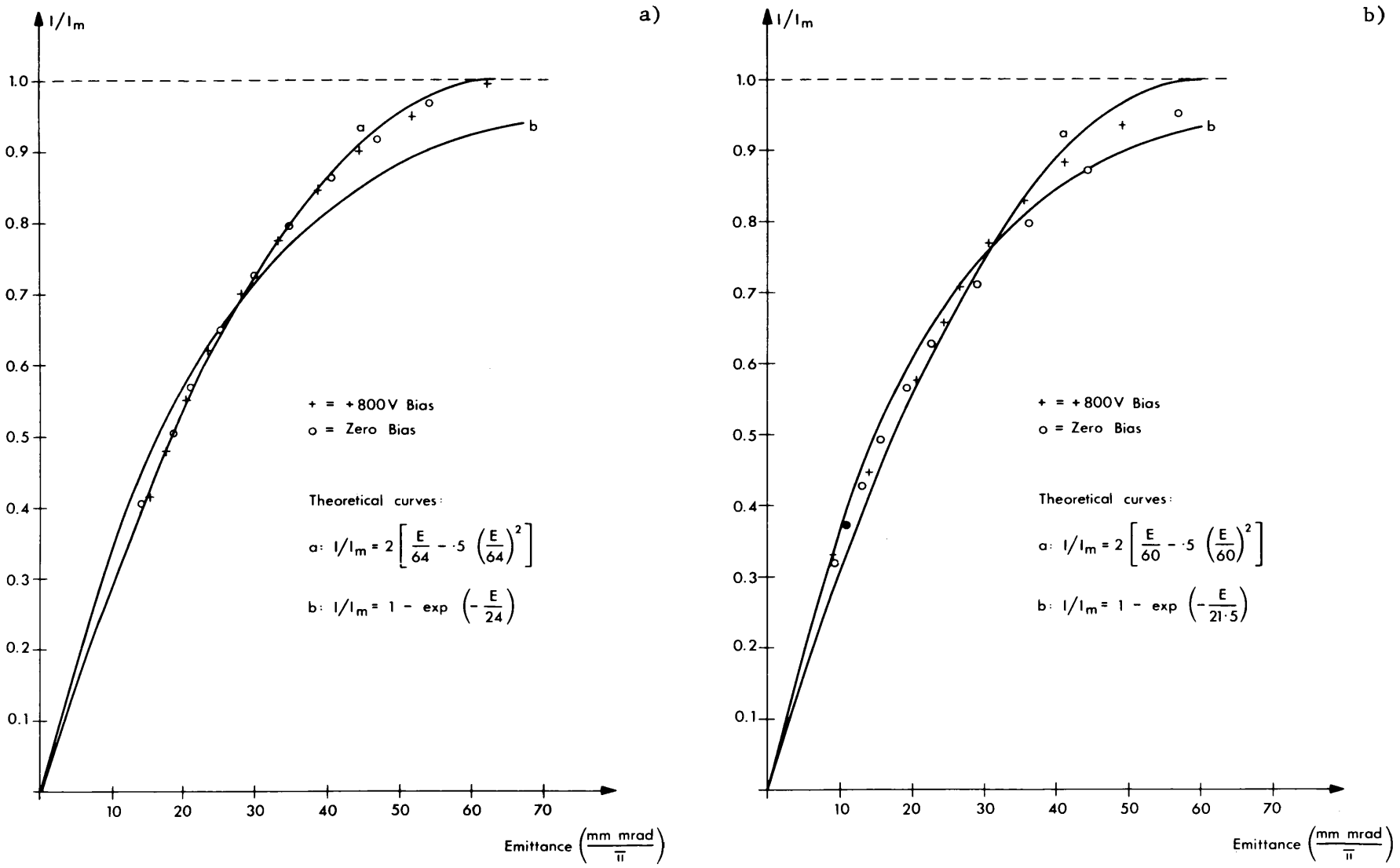

Fig. 7 Current versus emittance curves with and without bias: a) for Y-Y′ plane; b) for Z-Z′ plane